# See-through Image Quality Evaluation Index for Transparent Displays Considering Human Visual Sensitivity

*ChingLung Luo, MingHuang Chen, ChihLung Lin, ChiaHao Tsai, YungHsun Wu, ChiuLien Yang*

**Innolux Corporation, Miaoli, Taiwan**

## Abstract

***As transparent displays become more prevalent, assessing the quality of see-through images is increasingly important. Currently, no standard metrics exist for this purpose. We introduce a novel method that generates a human visual simulation image by CSPSF and convolving it with the background image. The simulated image is compared to the original using the SSIM Index. The robustness and validity of our proposed evaluation metric, termed the CROSS index, are substantiated through human visual perception scores, achieving a Kendall correlation coefficient of 0.929, thereby affirming its reliability and potential applicability in the field.***

## Author Keywords

CSF; PSF; SSIM; transparent displays; diffraction; image quality.

## 1. Introduction

The rapid development of transparent display technologies in fields like retail and smart homes has brought challenges in brightness, contrast, and cost. A key issue is the quality of see-through images, affected by the transparency aperture. Diffraction from the aperture matrix can blur images. Image quality is influenced by pixels per inch (PPI), aperture ratio, and aperture shape. Higher PPI increases diffraction, while a higher aperture ratio reduces it. Optimizing aperture shape and arrangement can also reduce diffraction [1-2].

Previous studies have introduced several metrics for evaluating the quality of see-through images, including haze, clarity, and ZOT (zero-order transmittance) [3], as well as Purity, which focuses on the energy ratio inside and outside a 0.2-degree field of view [4]. Additionally, the Structural Similarity Index (SSIM) is an important metric in image quality assessment, used to quantify the similarity between the original and blurred see-through images. SSIM considers factors such as luminance, contrast, and structure. However, when capturing photos before and after placing a see-through display, slight movements of the camera can affect the accuracy of the SSIM index. To address this, Multi-Scale Structural Similarity (MS-SSIM) [5] and Complex Wavelet SSIM (CW-SSIM) [6] have been developed to minimize the effects of slight shifts in the images being compared. MS-SSIM extends SSIM to multiple scales to evaluate image similarity at different levels, while CW-SSIM employs complex wavelet transforms with multi-sampling and filtering to improve robustness against geometric distortions.

However, the existing metrics do not account for the human visual system's sensitivity to various spatial distributions. We propose a novel simulation methodology that leverages Barten's contrast sensitivity function (CSF) [7] to refine the point spread function (PSF). This refined approach results in a new convolution kernel termed as the contrast sensitivity point spread function (CSPSF), which is used to create a CSF-corrected simulated diffraction image. The SSIM Index is then utilized to assess the similarity between this simulated image and the actual image, leading to the development of the contrast refined optical structural score (CROSS) index. To validate this methodology, human visual perception experiments were conducted.

## 2. Simulation Method

The diffraction pattern of light through a transparent aperture array can be analyzed using Fourier optics [8]. The Fraunhofer diffraction approximation is valid when $Z > \frac{2D^2}{\lambda}$. Under these conditions, the field distribution can be approximated by the Fourier transform of the aperture's field distribution [9], as shown in Equation 1. This approximation is crucial for determining the PSF, which characterizes the response of optical systems, including the human eye, to a point source.

$$E(X,Y) = F\{A(x,y)\} \tag{1}$$

Where, $A(x,y)$ represents the transparent aperture distribution, typically assigned a value of 1 for transmission and 0 for obstruction. The resultant $E(X,Y)$ is the far-field diffraction pattern generated by this transformation. The intensity distribution is obtained by squaring the magnitude of $E(X,Y)$. In this study, a Fourier transform is applied to a simulated 4×4 pixel aperture design with a 1-micron resolution. Figure 1(a) depicts the simulation aperture image, while Figure 1(b) shows the far-field diffraction pattern. Some of the central energy is spread into higher-order terms, causing a blurring effect in the see-through image.

However, to generate true image colors, it's important to consider wavelength variations, which primarily affect the diffraction angle. By adjusting the PSF, a comprehensive wavelength range is covered, ensuring that color representation is accurate across the spectrum. Furthermore, the eye's angular resolution suggests a need to reduce the resolution of the intensity distribution. This is achieved by initially interpolating to a finer resolution and then averaging to a more practical scale, which aligns with the eye's ability to discern detail.

The CSF reflects the human eye's varying sensitivity to luminance differences across different angular distances. Research indicates that the contrast sensitivity changes with special frequencies. A CSF incorporating directional contrast sensitivity is utilized, as noted in Equation 2. This approach adjusts the original PSF according to the human eye's directional contrast sensitivity, resulting in a contrast-corrected point spread function, termed CSPSF.

$$CSF(f_s) = \frac{5200\exp(-0.0016 f_s^2(1+\frac{100}{L_o})^{0.08})}{(1+\frac{144}{F^2}+0.64(1+3\sin^2(2\theta))f_s^2)(\frac{63}{L_o^{0.83}}+\frac{1}{1-\exp(-0.02 f_s^2)})} \exp\left(-\frac{\ln^2(\frac{L_s}{L_o}(1+\frac{144}{F^2})^{0.25}) - \ln^2((1+\frac{144}{F^2})^{0.25})}{2\ln^2(32)}\right) \tag{2}$$

where, $CSF(f_s)$ represents the CSF of the human eye, $f_s$ denotes the spatial frequency measured in cycles per degree. The parameter $L_o$ indicates the object luminance, while $L_s$ represents the ambient


ISSN 0097-996X/25/5602-0752-$1.00 © 2025

luminance, both expressed in candelas per square meter (cd/m²). The variable $F$ refers to the visual field of view (FOV), measured in degrees, and $\theta$ represents the angle of orientation.

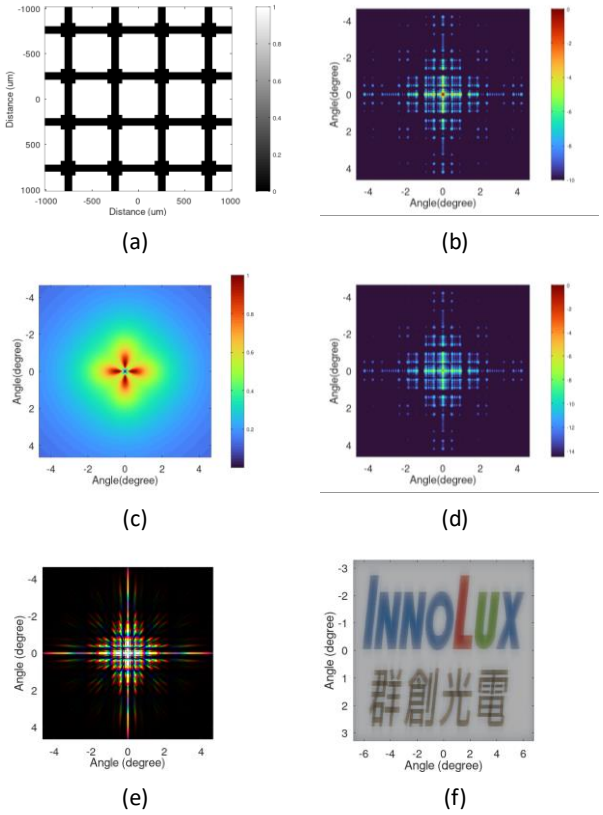


**Figure 1.** (a) Matrix of transparent aperture for simulation. Comparison of single-wavelength PSF before (b) and after (d) CSF correction. (c) CSF weight distribution used to correct PSF. (e) Realistic multi-wavelength PSF covering 400 to 700 nm. (f) Simulated diffraction image with a FOV of approximately 6.5 × 13.5 degrees.

Figure 1 (b, d) presents a comparison of the PSF before and after CSF correction. After correction, both low and high frequencies become less perceptible to the human eye. The FOV is approximately 9.3 × 9.3 degrees, and due to hardware limitations, the energy at larger angles is minimal and can therefore be neglected. As shown in Figure 1(c), the CSF is particularly sensitive to horizontal and vertical directions, while other directions exhibit varying contrast sensitivity according to the factor $1+3\sin^2(2\theta)$ .With the CSF correction, the PSF becomes more comprehensible within the system from the retina to the observed object.

The subsequent step involves weighting and summing the multi-wavelength CSPSFs using the color matching functions to accurately simulate the visual system's response in terms of tristimulus. These CSPSFs, corresponding to the tristimulus values, serve as convolution kernels to process the image of the scene situated behind the transparent display, thereby generating a diffraction-simulated image. Figure 1(e) illustrates the multi-wavelength CSPSFs, while Figure 1(f) presents the resultant simulated diffraction image. The generated diffraction image and the original image are used to calculate an SSIM index, and this comprehensive method is designated as the contrast refined optical structural score (CROSS) index. To assess the effectiveness of the CROSS index, it is compared with other established image quality indices and human perception ranking scores.

## 3. Visual Perception Assessment Experiment

Validation through human visual perception is essential to ensure the feasibility of the simulation methods and evaluation metrics. The visual perception experiment setup is detailed as follows: the optical arrangement is depicted in Figure 2. The camera is positioned 115 cm away, with a 15 cm distance to the transparent sample and a 100 cm distance from the sample to the object. The transparent sample used is chromium-coated quartz glass.

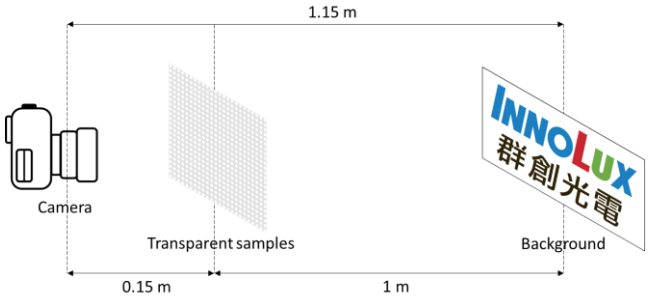


**Figure 2.** Setup of the visual perception experiment.

Considering the sensor's spatial resolution and the camera's focal length, the sensor's angular resolution is finer than that of the human eye. To better approximate visual perception, the camera-captured data is binned to more closely match the eye's angular resolution.

Figure 3 shows the graphical user interface (GUI) used in a visual perception experiment. The test was conducted on a 27-inch LCD screen with a resolution of 1920×1080 pixels, positioned 0.8 meters from the participants. Twenty individuals with normal or corrected vision participated. The test involved 13 samples, with 2 randomly selected each time, allowing for a maximum of 78 combinations. These 13 samples have aperture shapes similar to Figure 1 (a), but differ in PPI and aperture ratios, which are detailed in Table 1. Participants evaluated and chose among three options: the left image is clearer, the right image is clearer, or both images are the same. Theses comparisons result in a final human visual ranking of the 13 diffracted images. The image ranked last receives a score of 0, the second-to-last a score of 1, and so forth. Tied positions receive the same score. Scores are then normalized to ensure a consistent distribution range for all participants.

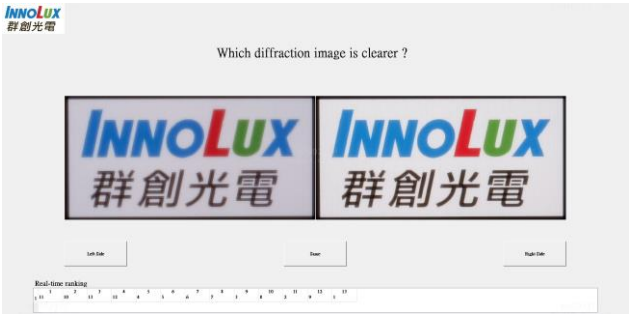


**Figure 3.** GUI for the visual perception experiment.

Additionally, eight samples were prepared and subjected to the same procedure. Unlike before 13 samples, these samples have a fixed 53 PPI and a fixed 68% aperture ratio, with each sample featuring a different aperture shape, as shown in Figure 4.

**Table 1.** Conditions of samples in visual perception Experiment 1.

| Sample | PPI | Aperture Ratio (%) | Sample | PPI | Aperture Ratio (%) |
|---|---|---|---|---|---|
| 1 | 53 | 20 | 8 | 200 | 68 |
| 2 | 53 | 40 | 10 | 25.4 | 83.67 |
| 3 | 53 | 60 | 10 | 33.87 | 78.25 |
| 4 | 53 | 80 | 11 | 50.8 | 67.46 |
| 5 | 50 | 68 | 12 | 84.67 | 46.05 |
| 6 | 80 | 68 | 13 | 101.6 | 35.42 |
| 7 | 100 | 68 | | | |

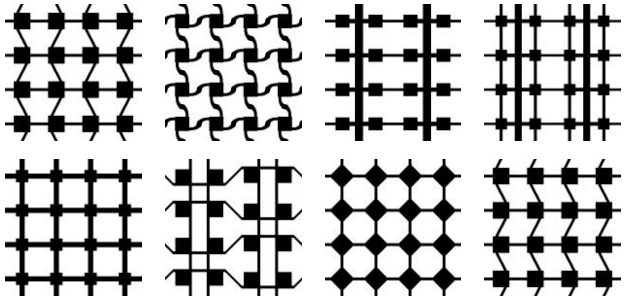

**Figure 4.** Different aperture shapes of samples in visual perception Experiment 2.

## 4. Correlation between Evaluation Metrics and Visual Perception Assessment

In this section, we validate the correlation between various image quality indices and the human ranking score, known as the mean opinion score (MOS). The MOS is derived from the rankings assigned by participants to the samples, represents the average score given by human evaluators. Experiments were conducted for optical metrics of haze and clarity, and simulations were performed for Purity, MS-SSIM, CW-SSIM and CROSS. The relations between each evaluation metric and MOS are illustrated in Figure 5-6.

The Kendall correlation coefficient is used to evaluate how good the relationship is between these metrics and visual perception. The key focus of the Kendall correlation coefficient is the rank consistency between two variables [10]. It involves calculating the number of concordant and discordant pairs and determining their correlation by computing the probability of consistency. The results of the Kendall correlation coefficient for each evaluation metric in relation to visual perception are presented in Table 2.

It is evident that the optical metric haze does not provide effective evaluative capability, as it primarily focuses on the energy distribution within and beyond 2.5 degrees. Clarity only considers narrow-angle scattering energy at the direct viewing angle, and human vision is not fully sensitive to low and high frequencies. Therefore, it is crucial to consider the frequency range that accurately simulates visual perception. Additionally, visual perception is sensitive to differences in brightness, a sensitivity that optical metrics lack. Although Purity offers a reasonable degree of correlation, with a Kendall correlation coefficient of 0.897, it shows several instances of significant conflict with visual perception, indicating a lack of comprehensive performance. In comparison, the CROSS, which is also based on SSIM, along with the advanced SSIM-based versions MS-SSIM and CW-SSIM, all demonstrate a high degree of correlation, with Kendall correlation coefficients greater than 0.92.

In Experiment 2, the conditions became more stringent, making the evaluation more challenging by altering the shape of the transparent aperture while keeping the PPI and aperture ratio constant. Clarity remained at the same level, and haze received a good score with a Kendall correlation coefficient of 0.857. Visual perception was evaluated in scenarios where the PPI and aperture ratio remained the same, but aperture shapes differed. This made the PSF stayed in the same angular range, which allowed haze to achieve a favorable quality assessment. Unfortunately, the Kendall correlation coefficient for Purity was only 0.789. This may be because Purity only considers energy within 0.2 degrees and does not adequately account for the appropriate frequency range for visual perception. As for CW-SSIM, it yielded unsatisfactory results, with a Kendall correlation coefficient of 0.643. This outcome may attributed to the down-sampling process inherent in CW-SSIM, which results in a loss of image detail and subsequently impairs the metric's discriminative capability. Meanwhile, MS-SSIM maintained a decent Kendall correlation coefficient of 0.857. However, CROSS achieved a Kendall correlation coefficient of 0.929, further confirming the stability and superiority of this evaluation approach.

CROSS enhances visual perception accuracy by using the CSPSF as a convolution kernel. This adjustment increases the weight of mid-range frequencies in the PSF while reducing the emphasis on low and high frequencies, which significantly aids in simulating visual perception. Furthermore, the CSPSF accounts for directional sensitivity, enhancing sensitivity in the horizontal and vertical directions while reducing sensitivity at oblique angles. This variation follows the factor $1 + 3\sin^2(2\theta)$, and the adjustment of directional weights greatly enhances realism.

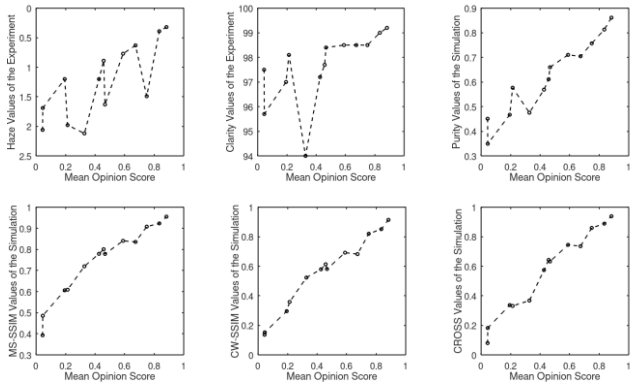


**Figure 5.** The MOS in experiment 1 corresponds to various evaluation metrics.

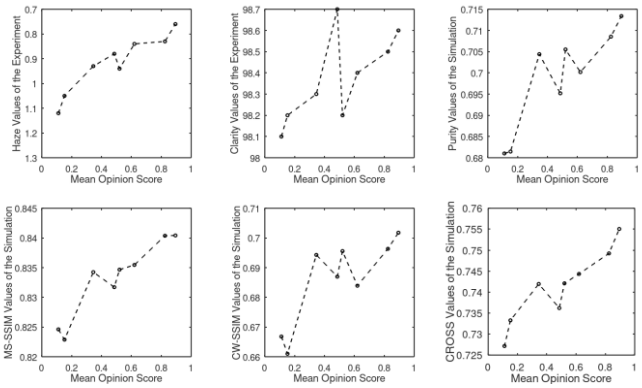


**Figure 6.** The MOS in experiment 2 corresponds to various evaluation metrics.

**Table 2.** (a) The Kendall correlation between various evaluation metrics and visual perception in Experiment 1, and (b) the Kendall correlation in Experiment 2.

| Evaluation Metrics | Haze | Clarity | Purity | MS-SSIM | CW-SSIM | CROSS |
|---|---|---|---|---|---|---|
| Kendall's Correlation | 0.632 | 0.745 | 0.897 | 0.923 | 0.949 | 0.923 |

(a)

| Evaluation Metrics | Haze | Clarity | Purity | MS-SSIM | CW-SSIM | CROSS |
|---|---|---|---|---|---|---|
| Kendall's Correlation | 0.857 | 0.618 | 0.789 | 0.857 | 0.643 | 0.929 |

(b)

## 5. Conclusion

To evaluate the visual image quality through a see-through display, traditional optical indices like haze, clarity or purity might misses detailed information within certain angular ranges of light distribution. This can make them less aligned with human perception, especially considering different PPI or aperture ratios of transparent displays. SSIM-based indices better align with human perception rankings. By adjusting the PSF with the human CSF, the CSPSF accounts the human eye's sensitivity to the spatial frequencies of the PSF. The CROSS provides results more consistent with human perception when testing pixels with same PPI and aperture ratio but with different aperture shapes. Notably, the CROSS achieved a high Kendall correlation coefficient of 0.923 and even reached 0.929 compared to the human ranking in tests with different pixel groups. This index significantly enhances the robustness of assessments regarding aperture variations, thus providing a reliable framework for image quality evaluation in the development of future transparent display panels. The high accuracy of image quality assessment achieved through simulation also streamlines the design process, fostering rapid advancements in transparent display technology.

## 6. References

1. Tsai YH, Huang MH, Jeng W, Huang TW, Lo KL, Mang Ou-Yang. Image quality affected by diffraction of aperture structure arrangement in transparent active-matrix organic light-emitting diode displays. Applied optics. 2015 Aug 28;54(28):E136–6.
2. Yang Q, Yang Z, Lan Y, Wu S. Low-diffraction transparent micro light-emitting diode displays with optimized pixel structure. Journal of the Society for Information Display. 2022 Apr 1;30(5):395–403.
3. Wang Z, Chi L, Chang Y, Xu X, Qiu J, Helander M. 54-2: Diffraction Issues of Under Display IR Sensor in AMOLED Displays. SID Symposium Digest of Technical Papers. 2024 Jun 1;55(1):738–41.
4. Kwon HJ, Lee SB, Lim K, Kang DW, Jun W, Yoon SY. 89-3: Invited Paper: An Investigation of Quantitative Measure of See-Through Image Quality for Transparent Displays. SID Symposium Digest of Technical Papers. 2024 Jun;55(1):1238–41.
5. Qin Z, Xie J, Lin FC, Huang YP, Shieh HPD. Evaluation of a Transparent Display's Pixel Structure Regarding Subjective Quality of Diffracted See-Through Images. IEEE Photonics Journal. 2017 Aug;9(4):1–14.
6. Tsai Y, Wu J, Huang M, Tien K, Fang Y. 89-2: An Evaluation Index for See-Through Image Quality on Transparent MicroLED Displays. SID Symposium Digest of Technical Papers. 2024 Jun 1;55(1):1234–7.
7. Barten PGJ. Formula for the contrast sensitivity of the human eye. Miyake Y, Rasmussen DR, editors. Image Quality and System Performance. 2003 Dec 19;
8. Goodman JW. Introduction to Fourier Optics. McGraw-Hill Science, Engineering .Mathematics; 1996.
9. Hecht E. Optics. San Francisco Addison-Wesley; 2010.
10. Kendall MG. A new measure of rank correlation. Biometrika. 1938;30(1-2):81-93.